J Am Oil Chem Soc (2011) 88:1977–1987
DOI 10.1007/s11746-011-1871-3

ORIGINAL PAPER

Fuel Properties of Biodiesel/Ultra-Low Sulfur Diesel (ULSD) Blends

Robert O. Dunn

Received: 13 October 2010 / Revised: 18 February 2011 / Accepted: 27 May 2011 / Published online: 17 June 2011

Abstract Biodiesel is an alternative fuel and fuel extender easily derived from vegetable oil or animal fat. In 2006, the US Environmental Protection Agency mandated that maximum sulfur content of diesel fuels be reduced to 15 ppm to protect catalysts employed in exhaust after-treatment devices. Processing to produce this ultra-low sulfur petrodiesel (ULSD) alters fuel lubricity, density, cold flow, viscosity, and other properties. Consequently, there is a need to develop a better understanding of the basic fuel properties of biodiesel/ULSD blends. This work evaluates the effects of biodiesel volumetric blend ratio (V_{BD}) on cloud point (CP), kinematic viscosity (v), specific gravity (SG), and refractive index (RI) of blends with petrodiesel. Properties measured for various blends of methyl esters of soybean oil (SME) and used cooking oil (UCOME) in ULSD were compared with those for blends with low sulfur (≤500 ppm) petrodiesel fuel (LSD). With respect to increasing V_{BD}, CP and SG increased and RI decreased with each parameter demonstrating a linear correlation. In contrast, v showed a curvilinear relationship with respect to increasing V_{BD}. Calibration curves were derived from regression analyses to determine V_{BD} in biodiesel/ULSD blends from measurements of each individual property. While the models had generally high coefficients of regression ($R^2 > 0.986$), SG models were most accurate for predicting V_{BD} to within 1.3 vol%.

Keywords Biodiesel · Blend ratio · Cloud point · Refractive index · Specific gravity · Kinematic viscosity

Introduction

Biodiesel is a renewable alternative fuel made primarily from transesterification of plant oils or animal fats with methanol or ethanol. The National Biodiesel Board estimates that 700 million gallons (1 US gallon is approx. 3.79 liters) of biodiesel were produced in the US in 2008 [1]. Biodiesel has been applied to fuel transportation trucks, farm and other off-road vehicles, automobiles, locomotives, aircraft, stationary power generators, boilers, and heaters.

Biodiesel possesses many characteristics that make it attractive as an alternative fuel for conventional diesel (petrodiesel). It is readily biodegradable, non-toxic, and non-flammable making it easier to store and handle. Gross heats of combustion, specific gravity (SG), and viscosity are comparable to those properties of petrodiesel. Biodiesel is miscible with petrodiesel and enhances cetane number, lubricity, and anti-wear properties [2–6]. It can be applied as a fuel component where its volumetric ratio (V_{BD}) is above 20 vol% (B20), an extender ($V_{BD} \leq$ B20) or an additive ($V_{BD} \leq$ B5) in blends with petrodiesel. Biodiesel reduces exhaust emissions with respect to smoke opacity, hydrocarbons, carbon monoxide, sulfur dioxide, polyaromatic hydrocarbons, and particulate matter [2, 3, 5, 7]. Blends with biodiesel may increase nitrogen oxides (NOx) emissions, though increases do not exceed 5% for V_{BD} up to B20 [7]. A recent "well-to-wheel" life-cycle analysis reported that biodiesel has an energy output/fossil energy

Mention of trade names or commercial products in this publication is solely for the purpose of providing specific information and does not imply recommendation or endorsement by the US Department of Agriculture. USDA is an equal opportunity provider and employer.

R. O. Dunn (✉)
Bio-Oils Research, United States Department of Agriculture (USDA), Agricultural Research Service (ARS), National Center for Agricultural Utilization Research, Peoria, IL, USA
e-mail: Robert.Dunn@ars.usda.gov

input ratio of 4.56:1 [8]. Another study [9] showed that biodiesel from soybean oil reduces green house gas (carbon monoxide, methane and nitrous oxide) emissions by 66–94% depending on how co-products (glycerol) are addressed after conversion.

In 2006, the US Environmental Protection Agency (USEPA) mandated that sulfur levels in on-road transportation diesel fuels be no greater than 15 ppm to prevent poisoning of catalysts used in devices designed to treat particulate matter and NOx in exhaust emissions [1]. To meet this specification, the petroleum industry upgrades petrodiesel by catalytic reaction with high-pressure hydrogen to remove sulfur and other heteroatoms [10]. The resulting product is generally referred to as ultra-low sulfur diesel (ULSD) to distinguish it from its low sulfur diesel (LSD; sulfur content $\leq$ 500 ppm) predecessor.

Hydrotreating the petroleum distillate product modifies other fuel properties. Although fuel lubricity and anti-wear properties are diminished after processing, these characteristics can be restored by blending ULSD with 1–2 vol% biodiesel [11]. Other properties that may be affected include cetane number, cloud point (CP), cold filter plugging point, pour point, SG, and kinematic viscosity (ν). It follows that blending biodiesel with ULSD will have variations in fuel properties relative to blends with LSD.

Although some fuel property data are available for non-blended (neat) biodiesel and ULSD in the scientific literature, data pertaining to blends with specified volumetric ratios (V_{BD}) is relatively scarce. Tang and coworkers [12, 13] studied the effects of blending ULSD with biodiesel from several feedstocks on stability during storage in cold temperatures. This work showed that CP of blends was correlated to V_{BD} by second-order polynomial equations [12]. In contrast, another report [14] showed that CP increased linearly with respect to increasing V_{BD} for biodiesel in blends with No. 2 ULSD. Blends with winter ULSD or No. 1 ULSD demonstrated curvilinear behavior at V_{BD} below B20. Knothe and Steidley [15] studied the effects of low temperatures on ν of soybean oil-fatty acid methyl esters (SME)/ULSD blends. Data interpreted in that work demonstrated a curvilinear relationship between ν at 40 °C and V_{BD} of blends.

Despite the aforementioned examples, most of the fuel property data reported in the scientific literature pertain to blends of biodiesel and LSD. To increase the fundamental understanding of the properties of biodiesel/ULSD blends, establishing an adequate baseline will require acquisition, analysis, and reporting of more data. The first objective of the present study addresses this concern by comparing measured CP, refractive index (RI), SG, and ν results and evaluating differences between blends of SME and used cooking oil-fatty acid methyl esters (UCOME) in LSD and ULSD.

Verifying biodiesel blend ratio levels (V_{BD}) is important since government tax credits or other regulatory issues may depend on them. A quality survey on biodiesel/petrodiesel blends was conducted in Michigan where blend levels were determined by gas chromatography (GC)/mass spectrometry [16]. This study found that B0 blends had as much as 3 vol% biodiesel, levels that are now acceptable under the American Society of Testing and Materials (ASTM) specification D 975 for diesel fuel oils [17]. However, 4 of 19 different B20 samples were found to contain no more than 10 vol% biodiesel.

Laboratory methods have been developed that generally require expensive instruments and equipment to perform. An early report [18] recommended high performance liquid chromatography (HPLC) coupled with a mass-sensitive detector, such as an evaporative light scattering detector (ELSD), over GC analysis with a flame ionization detector. The latter technique produces complex chromatograms owing to the number and diversity of compounds found in petrodiesel [19]. HPLC with ELSD or ultraviolet (UV) absorption detection was reported to analyze biodiesel blends with B1–B30 blend ratios [20]. Simultaneous determination of fatty acid methyl ester (FAME) and aromatics in blends was conducted by HPLC with RI and UV detectors [21].

Direct determination of blend levels in biodiesel/petrodiesel blends can also be made from infrared (IR) spectra [22]. Partial least-squares (PLS) models based on IR or near-IR spectra were shown to identify blend levels below B5 [23]. Near-IR and ^{1}H-nuclear magnetic resonance (NMR) spectroscopy were compared for determining blend levels for all ranges (B0–B100) in SME/LSD blends [24]. Predicted values were within 1–1.5% of measured values, though near-IR was more accurate for V_{BD} below B30. Fourier transform-IR (FT-IR) was utilized to identify chemical group structures in biodiesel as well as determine blend levels of FAME derived from a diverse number of lipid feedstocks [25]. ASTM test method D 7371 employs FT-IR/attenuated total reflectance/PLS to determine blend levels of biodiesel in petrodiesel. This method is referenced in ASTM fuel specification D 7467 for biodiesel/diesel fuel oil blends (B6–B20) [26].

Instruments and equipment necessary to carry out in-house analyses of blend levels by HPLC, near-IR, mid-IR, or ^{1}H-NMR spectroscopic methods are expensive. One cheaper option is to send samples to contract labs and await the results to verify blend levels. A more practical alternative may be to develop calibrations based on fuel properties that may be measured with less expensive and/or performed utilizing portable equipment. Therefore, the second and main objective of the present study was to devise calibration curves based on CP, RI, SG, and ν for determining blend levels in blends of SME and UCOME in ULSD.

Experimental Methods

Materials

Firm names of sources for supplying two SME samples, denoted 'SME-1' and 'SME-2', and the UCOME sample are not provided to remove bias in presenting and interpreting the results. All three biodiesel samples were stored in a dark refrigerator when not in use. An earlier study [27] reported acid value $\leq$ 0.22 mg KOH/g, free glycerol $<$ 0.02 mass%, total glycerol $<$ 0.1 mass%, and water content $\leq$ 480 ppm for SME-1 and SME-2. UCOME had acid value = 0.6 mg KOH/g, free glycerol = 0.003 mass%, total glycerol = 0.09 mass%, and water content = 476 ppm. Thus, only the acid value of UCOME among these data slightly exceeded the limit referenced in ASTM specification D 6751 for biodiesel [28].

Amoco standard No. 2 low sulfur petrodiesel (LSD2) with sulfur content $\leq$ 500 ppm was provided by the University of Illinois (Urbana, IL, USA). ULSD (sulfur content $\leq$ 15 ppm) samples were acquired from two separate sources. 'ULSD-A' was provided by the University of Idaho (Moscow, ID, USA) and Standard No. 2 'ULSD-B' was from Chevron USA (San Ramon, CA, USA). None of the petrodiesel samples contained performance-enhancing additives. Reverse osmosis filtered water was available in-house.

Methods

Fatty acid methyl ester (FAME) compositions were determined with a Varian (Walnut Creek, CA) model 8400 GC equipped with a flame ionization detector and a Supelco (Bellafonte, PA) SP2380 GC column (30 m × 0.25 mm i.d.). Carrier gas was helium at 1 mL/min. The temperature program was as follows: (1) hold at 150 °C for 15 min; (2) increase at 2 °C/min to 210 °C; (3) increase at 50 °C/min to 220 °C; and (4) hold at 220 °C for 5 min. Injector and detector temperatures were 240 and 270 °C. Individual FAME were identified by peak retention time and quantified by peak area. Results from analysis of SME-1, SME-2, and UCOME are shown in Table 1.

Cloud point (CP) data were measured in a PSA-70S automatic analyzer from Phase Technology (Richmond, BC, Canada) according to ASTM standard test method D 5773 [29]. RI data were determined in a Reichert Mark II Plus Abbe refractometer from Fisher Scientific (Pittsburgh, PA, USA) applying ASTM method D 1218 [30]. Samples were analyzed at room temperature (22–24 °C) and results automatically adjusted to yield RI at 25 °C. SG data at 15.6 °C referenced to water at the same temperature were measured in laboratory pycnometers according to American Oil Chemists' Society (AOCS) method Cc 10c-95 [31]. Kinematic viscosity (ν) data were measured at 40 °C in Cannon–Fenske (State College, PA, USA) capillary viscometers and applying ASTM method D 445 [32].

Biodiesel/petrodiesel blends at different V_{BD} were prepared by pipetting precisely measured volumes and gently mixing contents at room temperature (22–24 °C). Properties were measured at V_{BD} = B0, B1, B2, B3, B4, B5, B8, B12, B16, B20, and B100 (0, 1, 2, 3, 4, 5, 8, 12, 16, 20, and 100 vol%) biodiesel in blends with petrodiesel. Subsets of data for each biodiesel/petrodiesel blend were analyzed by least-squares regression to yield calibration curves of the form V_{BD} versus CP, SG, RI, or ν. Modeling and statistical analyses were performed in MicroSoft (Redmond, WA, USA) Excel® spreadsheets.

Results and Discussion

FAME composition profiles of the three biodiesel fuels are summarized in Table 1. SME-1 and SME-2 had similar profiles with the latter having slightly more total unsaturated FAME content (ΣUnsat). In contrast, UCOME had significantly higher total saturated FAME content (ΣSat) and lower polyunsaturated FAME (C18:2 and C18:3) content than either SME. Furthermore, nearly one-fifth of the monounsaturated C18:1 FAME in UCOME was composed of the *trans* isomer, methyl elaidate. This isomer has a significantly higher melting point than the *cis* isomer, methyl oleate [33]. The *trans* isomers most likely formed in the feedstock cooking oil either as a result of partial hydrogenation to stabilize it or during its use at high temperatures in food preparation. The relatively high *trans* isomer concentration carried through after conversion of used cooking oil into biodiesel.

Results from analysis of CP, RI, SG, and ν of neat (unblended) SME-1, SME-2, UCOME, LSD2, ULSD-A, and ULSD-B are listed in Table 2. Effects of variations in the FAME profile between SME and UCOME are reflected in both CP and ν data. The higher ΣSat and methyl elaidate content in UCOME caused its CP to be significantly higher than SME. Higher ΣSat are also known to increase ν [15], an effect that is reflected in data shown in Table 2. RI data for biodiesel were grouped in a lower range (1.452–1.456) than those for petrodiesel (1.459–1.472). Similarly, SG data for biodiesel were grouped in a higher range (0.882–0.889) compared to petrodiesel (0.826–0.850).

While RI and ν were generally comparable for ULSD-A and ULSD-B, significant deviations were observed in CP and SG data. The most likely explanation is that ULSD-A was a mixture of No. 1 and No. 2 ULSD fuels, sometimes referred to as winter ULSD. This procedure is generally done to lower CP for cold weather operations. Hence, the CP of ULSD-A is more than 10 °C lower than that of

Table 1 Fatty acid concentration profile of biodiesel fuels analyzed by gas chromatography (GC)

Biodiesel	FAME (wt%)								
	C14	C16	C16:1	C18	C18:1	C18:2	C18:3	ΣSat	ΣUnsat
SME-1	nd	12.5	nd	4.3	24.2	51.5	7.6	16.8	83.2
SME-2	nd	11.0	nd	4.3	21.7	54.5	8.5	15.3	84.7
UCOME	0.6	15.3	0.9	8.1	49.0[a]	24.0	2.2	24.0	76.0

FAME Fatty acid methyl esters, *C14* myristate, *C16* palmitate, *C16:1* palmitoleate, *C18* stearate, *C18:1* oleate, *C18:2* linoleate, *C18:3* linolenate, *ΣSat* total saturated FAME content, *ΣUnsat* total unsaturated FAME content, *UCOME* used cooking oil-FAME, *SME* soybean oil-FAME, *nd* not detected

[a] 10.4 wt% C18:1-*trans* isomer (elaidate)

Table 2 Cloud point (CP), refractive index (RI), specific gravity (SG), and kinematic viscosity (ν) of unblended biodiesel and petrodiesel fuels

Fuel	CP (°C)	RI at 25 °C	SG at 15.6 °C	ν at 40 °C (mm^2/s)
SME-1	0.5 ± 0.49	1.4563 ± 3.0E−04	0.889 ± 1.1E−03	4.3 ± 0.21
SME-2	1.5 ± 0.13	1.4563 ± 5.7E−04	0.888 ± 1.5E−03	4.14 ± 0.018
UCOME	8.3 ± 0.10	1.4518 ± 3.0E−04	0.8824 ± 2.0E−04	4.84 ± 0.013
LSD2	−16.7 ± 0.18	1.47200 ± 9.5E−05	0.8502 ± 1.8E−04	2.702 ± 6.2E−03
ULSD-A	−26.6 ± 0.98	1.4587 ± 1.8E−04	0.82568 ± 9.1E−05	2.507 ± 6.4E−03
ULSD-B	−13.9 ± 0.21	1.468 ± 1.0E−03	0.8471 ± 9.2E−04	2.54 ± 0.060

LSD2 No. 2 low sulfur petrodiesel, *ULSD* ultra-low sulfur petrodiesel; see Table 1 for abbreviations

ULSD-B. Data in Table 2 also demonstrate that ULSD-A has significantly lower SG than ULSD-B, an effect that is consistent for mixtures of No. 1 and No. 2 petrodiesel fuels. Finally, CP, RI, and SG data for LSD2 and ULSD-B were comparable for these two forms of No. 2 petrodiesel.

Properties of Blends with LSD2, ULSD-A and ULSD-B

The graphs shown in Fig. 1 are CP, RI, SG, and ν data curves for blends with V_{BD} = B0, B1, B2, B3, B4, B5, B8, B12, B16, and B20 (vol%). For each property, data were collected for blends of SME-1 and SME-2 in LSD2, ULSD-A, and ULSD-B and blends of UCOME in LSD2 and ULSD-B. This generated 32 data curves in 12 separate graphs. To allow clarity in the presentation of results, one representative graph was selected for each property.

Figure 1a is a graph of CP results for SME-1 blends. CP increased linearly as V_{BD} increased from B0 to B100 (data above B20 not shown). As expected from comparison of CP data for unblended fuels in Table 2, blends with ULSD-A tend to have CP at significantly lower temperatures than blends with LSD2 and ULSD-B. CP results for ULSD-B blends were only 2.8 °C greater than those for LSD2 blends and deviation between these curves decreased as V_{BD} increased. Nearly identical trends were observed in CP curves for blends with SME-2 and UCOME.

Results for RI of SME-2 blends are shown in Fig. 1b. In this case, RI decreased linearly as V_{BD} increased from B0 to B100. Analogous to CP data, RI of blends with LSD2 and ULSD-B are closer to each other than for blends with ULSD-A. The maximum deviation in RI between LSD2 and ULSD-B curves was <0.003 whereas the ULSD-A curve was more than 0.01 lower. Increasing V_{BD} from B0 to B20 decreased RI by 0.004 and 0.002 for LSD2 and ULSD-B curves; however, the ULSD-A curve decreased by only 0.0008 over the same range in V_{BD}. Again, nearly identical trends were observed in RI curves for blends in SME-1 and UCOME.

Results for SG of SME-1 blends are given in Fig. 1c. Similar to CP results, SG increased linearly as V_{BD} increased from B0 to B100. Results for blends with LSD2 and ULSD-B were very close together (<0.003) in contrast to being more than 0.02 higher in range than SG of ULSD-A blends. All three blends exhibited substantial increases with increasing V_{BD} from B0 to B20. Nearly identical trends were observed in SG curves for blends with SME-2 and UCOME.

Finally, results for ν of SME-2 blends are shown in Fig. 1d. Each blend demonstrated some degree of curvature though it was more pronounced when comparing data for V_{BD} up to B100 (data above B20 not shown). In contrast to CP, RI, and SG data curves, results for blends with ULSD-A and ULSD-B were closer to each other than for blends with LSD2. Deviations between ν curves for ULSD-A and ULSD-B were in the range 0.05–0.11 mm^2/s whereas the ν curve for LSD2 blends was 0.15–0.18 mm^2/s above the ULSD-A curve. All three blends exhibited substantial increases with increasing V_{BD} from B0 to B20.

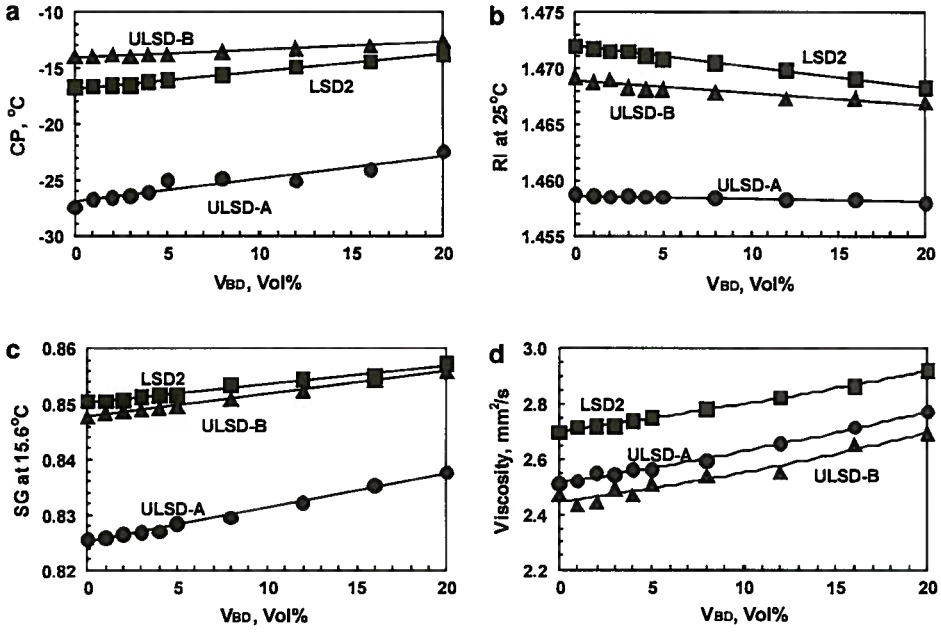

Fig. 1 Property versus blend ratio (V_{BD}) data for soybean oil-fatty acid methyl ester (SME) blends with No. 2 low sulfur petrodiesel (LSD2) and ultra-low sulfur petrodiesel ULSD-A and ULSD-B. **a** Cloud point (CP) of SME-1 blends (standard deviation [SD] $\leq$ 0.75); **b** refractive index (RI) at 25 °C of SME-2 blends (SD $\leq$ 0.00061); **c** specific gravity (SG) at 15.6 °C of SME-1 blends (SD $\leq$ 0.00041); and **d** kinematic viscosity (ν) at 40 °C of SME-2 blends (SD $\leq$ 0.031)

Nearly identical trends were observed in ν curves for blends with SME-1 and UCOME.

Calibration Curves for Predicting V_{BD} from Property Data

Based on results discussed above, calibration curves for predicting V_{BD} from measurements of CP, RI, SG, and ν were determined by least-squares integration. Thus, regression was performed with $y = V_{BD} = f(x)$ where x = a given property. CP, RI, and SG curves were analyzed by linear regression yielding equations of the form:

$$V_{BD} = A_0 + A_1 x$$

where A_0 and A_1 are constants (intercept and slope). Calibration curves based on this model were determined from regression of property data for blends with V_{BD} = B0, B5, B20, and B100 because these ratios are routinely encountered in the field. Second-order polynomial regression was performed on ν curves yielding equations of the form:

$$V_{BD} = A_0 + A_1 x + A_2 x^2$$

where A_0, A_1, and A_2 are constants. These calibration curves required more than four points to generate and property data measured for blends with V_{BD} = B0, B4, B8, B12, B16, B20, and B100 were utilized. Thus, regression analyses for the present work placed great emphasis on developing calibration curves based on data between B0 and B20 plus B100. Results for blends with ULSD-A and ULSD-B are summarized in Tables 3, 4, 5, 6.

CP Calibration Curves

A study discussed earlier reported that CP-V_{BD} data for biodiesel/ULSD blends were fitted by second-order polynomial expressions [12]. However, that study was performed on blends with ULSD whose CP = −25 °C, a value that is considerably lower than those of unblended ULSD-A or ULSD-B in the present study (Table 2). Another study [14] reported on the effects of blending biodiesel with ULSD formulated with CP-levels of −40, −34, −20, and −12 °C. Results showed that CP curves were linear with respect to V_{BD} for blends with ULSD at the highest CP-level while blends with lower CP-level ULSD tended to exhibit increases in curvilinear behavior especially for blends with V_{BD} below B20. Mixing No. 1 in No. 2 grade petrodiesel varies CP depending on volumetric concentration of No. 1 petrodiesel. Thus, it is likely the study [12] reporting the second-order relationship was performed on blends with winter ULSD.

For biodiesel blends with No. 2 petrodiesel, there is precedent in other studies supporting the behavior of CP results in the present study. Earlier reports [34, 35] showed that blends of SME and No. 2 LSD yielded linear relationships between CP and V_{BD}. More recently, Joshi and Pegg [36] reported nearly linear relationships for ethyl esters of fish oil blended with No. 2 petrodiesel. Benjumea et al. [37] demonstrated that blends with palm oil biodiesel followed a linear pattern based on Kay's mixing rule for binary mixtures.

Results shown in Fig. 1a suggested that a linear relationship may be employed to calculate V_{BD} as a function of

Table 3 Results from regression analysis of biodiesel volumetric blend ratio (V_{BD}) versus CP data

Biodiesel	n	A_0	Err	A_1	Err	F	R^2	σ_y
ULSD-A blends								
SME-1	4	97	2.8	3.5	0.13	733	0.9959	3.0
SME-2	4	94	2.4	3.5	0.11	978	0.9969	2.6
Combined SME	**8**	**95**	**2.0**	**3.56**	**0.092**	**1,486**	**0.9953**	**3.0**
ULSD-B blends								
SME-1	4	101	5.4	6.9	0.46	227	0.9869	5.3
SME-2	4	91	1.3	6.5	0.12	2,892	0.9990	1.5
Combined SME	**8**	**95**	**3.3**	**6.6**	**0.29**	**513**	**0.9865**	**5.0**
UCOME	4	63	2.8	4.5	0.24	343	0.9913	4.3

Linear regression based on CP results at V_{BD} = B0, B5, B20, and B100

n Number of observations, A_0 intercept, A_1 slope, *Err* error of the coefficient, F variance ratio (model/residuals), R^2 adjusted correlation coefficient, σ_y standard error of the y-estimate. See Tables 1 and 2 for abbreviations

Table 4 Results from regression analysis of biodiesel volumetric blend ratio (V_{BD}) versus RI data

Biodiesel	n	A_0	Err	A_1	Err	F	R^2	σ_y
ULSD-A blends								
SME-1	4	68,000	3,900	−46,000	2,700	297	0.9900	4.7
SME-2	4	53,000	3,200	−36,000	2,200	280	0.9894	4.8
Combined SME	**8**	**59,000**	**3,800**	**−40,000**	**2,600**	**239**	**0.9714**	**7.3**
ULSD-B blends								
SME-1	4	12,000	310	−8,200	210	1,514	0.9980	2.1
SME-2	4	12,000	430	−8,300	290	817	0.9963	2.8
Combined SME	**8**	**12,000**	**340**	**−8,200**	**230**	**1,249**	**0.9944**	**3.2**
UCOME	4	9,000	180	−6,400	120	2,873	0.9990	1.5

Linear regression based on RI results at V_{BD} = B0, B5, B20, and B100. See Tables 1, 2, and 3 for abbreviations

Table 5 Results from regression analysis of biodiesel volumetric blend ratio (V_{BD}) versus SG data

Biodiesel	N	A_0	Err	A_1	Err	F	R^2	σ_y
ULSD-A blends								
SME-1	5	−1,290	19	1,570	22	5,200	0.9992	1.4
SME-2	5	−1,340	15	1,630	18	8,584	0.9995	1.1
Combined SME	**10**	**−1,320**	**17**	**1,590**	**20**	**6,549**	**0.9986**	**1.8**
ULSD-B blends								
SME-1	4	−2,030	10	2,400	12	42,191	0.99993	0.39
SME-2	4	−1,990	33	2,350	39	3,674	0.9992	1.3
Combined SME	**8**	**−2,010**	**18**	**2,370**	**21**	**12,760**	**0.9995**	**1.0**
UCOME	4	−2,330	17	2,760	20	19,056	0.9998	0.58

Linear regression based on SG results at V_{BD} = B0, B5, B20, and B100 (two data points for ULSD-A blends). See Tables 1, 2, and 3 for abbreviations

CP. Linear regression results listed in Table 3 confirmed this observation for blends with ULSD-A and ULSD-B. Adjusted correlation coefficients (R^2) were > 0.986, variance ratios (F = variance of the model to that of the residuals) were ≥ 227 and standard errors of the y-estimate (σ_y) were 1.5–5.3.

Similarities between corresponding A_0 and A_1 coefficients for SME-1 and SME-2 blends strongly showed that data sets could be pooled to yield expressions for combined SME/ULSD blends (results shown in bold-face in Table 3). Results for the combined SME models compared well with individual SME/ULSD blends. On the other hand, A_0 and

Table 6 Results from regression analysis of biodiesel volumetric blend ratio (V_{BD}) versus ν data

Biodiesel	n	A_0	Err	A_1	Err	A_2	Err	F	R^2	σ_y
ULSD-A blends										
SME-1	7	−250	22	130	13	−11	1.8	5,081	0.9994	0.84
SME-2	7	−270	20	140	13	−12	1.9	9,704	0.9997	0.61
Combined SME	**14**	**−348**	**9.9**	**190**	**21**	**−19**	**3.1**	**1,456**	**0.9956**	**2.2**
ULSD-B blends										
SME-1	7	−350	46	190	29	−20	4.4	2,395	0.9987	1.2
SME-2	7	−280	71	150	45	−14	6.8	823	0.9964	2.1
Combined SME	**14**	**−310**	**42**	**170**	**27**	**−16**	**4.0**	**2,516**	**0.9974**	**1.7**
UCOME	7	−330	46	170	27	−18	3.7	1,361	0.9978	1.6

Second-order polynomial regression analysis based on ν results at V_{BD} = B0, B4, B8, B12, B16, B20, and B100

A_2 Second-order coefficient; see Tables 1, 2, and 3 for abbreviations

A_1 coefficients for UCOME/ULSD-B blends were significantly lower ($P < 0.01$) than coefficients for SME/ULSD-B blends.

RI Calibration Curves

Waynick [38] noted that RI is sensitive to fatty acid group oxidation and increases when the concentration of polymers increases during degradation. RI detectors coupled with HPLC analysis were utilized in determining FAME concentrations in blends [21]. Although an early report [35] confirmed a strong linear correlation ($R^2 > 0.999$) between RI and V_{BD} for SME/No. 2 LSD blends, extensive studies on RI of biodiesel/ULSD blends have not been reported.

Results in Fig. 1b demonstrated a linear relationship may be developed for calculating V_{BD} as a function of RI. Linear regression results from these calibrations for blends with ULSD-A and ULSD-B are shown in Table 4. The four-point calibrations yielded $R^2 \geq 0.989$ and F ratio ≥ 280. σ_y values were larger for ULSD-A blends (4.7 and 4.8) than for ULSD-B blends (1.5–2.8). With respect to ULSD, similarities between corresponding A_0 and A_1 coefficients for SME-1 and SME-2 blends showed these data sets may be pooled to yield combined SME/ULSD expressions (results shown in bold face).

Regression results for combined SME/ULSD-A blends resulted in decreasing R^2 to 0.97 with respect to results for non-pooled data. This was likely caused by relatively small decreases in RI correlated to increasing V_{BD} from B0 to B100 which produced very sharp A_1 coefficients (slopes). This means that predicting V_{BD} for SME/ULSD-A blends may be problematic depending upon the degree of variation in RI measurements. Combined SME/ULSD-B blends yielded curves with flatter slopes making the prediction of V_{BD} less dependent on slight variations in RI and resulting in $R^2 = 0.994$ and $\sigma_y = 3.2$. Similar to results for CP calibrations, A_0 and A_1 coefficients for UCOME/ULSD-B blends were significantly lower in absolute value ($P < 0.01$) than coefficients for SME/ULSD-B blends.

SG Calibration Curves

Fuel density (SG) is an important property that determines fuel efficiency and correlates with other performance factors. Many fuel producers and distributors base their schedules on the 'gravity' (SG or API) of the fuel based on components including biodiesel. An early study [35] reported a strong linear correlation ($R^2 = 0.999$) between SG at 15.6 °C and V_{BD} for SME/No. 2 LSD blends. Similar results were reported more recently for blends of biodiesel from six different vegetable oils and No. 2 petrodiesel [39].

Results in Fig. 1c showed that a linear relationship may be developed for calculating V_{BD} as a function of SG. Linear regression results from these calibrations for blends with ULSD-A and ULSD-B are summarized in Table 5. Two separate data points for neat (B100) SME-1 and SME-2 were included in regression analyses for blends with ULSD-A. All SG-based calibrations yielded excellent results with respect to $R^2 \geq 0.999$, F ratio $\geq 3{,}674$ and $\sigma_y \leq 1.4$.

With respect to ULSD, similarities between A_0 and A_1 coefficients for SME-1 and SME-2 blends strongly showed these data sets could be pooled to yield combined expressions for SME/ULSD blends. Results shown in bold face in Table 5 indicate that the regression for the combined SME data did not significantly compromise R^2, F ratio, or σ_y. Similar to results for RI calibrations, A_0 and A_1 coefficients for UCOME/ULSD-B blends were significantly higher in absolute value ($P < 0.001$) than coefficients for SME/ULSD-B blends.

Viscosity Calibration Curves

In terms of correlating ν of biodiesel/petrodiesel blends, semi-logarithmic functions based on concentration and ν of

unblended biodiesel and petrodiesel components are frequently applied [36, 37, 40]. However, equations of this form are difficult to rearrange to show V_{BD} as a function of v of the blend and an alternative empirical approach was deemed appropriate.

Schumacher et al. [35] reported a weak linear correlation ($R^2 \sim 0.962$) between V_{BD} and v for SME/No. 2 LSD blends. Linear regression based on four data points (B0, B5, B20, and B100) was initially applied in analysis of V_{BD} versus v data in the present study with results showing good degrees of linearity ($R^2 \geq 0.988$) and F ratio ≥ 248. However, σ_y values were 6.3 for combined SME/ULSD-A blend data and 5.1 for combined SME/ULSD-B data.

Observations made of graphical results such as those shown in Fig. 1d revealed noticeable curvilinear behavior in the data curves. Alptekin and Canakci [39] reported similar behavior for blends of biodiesel from six different vegetable oils with No. 2 petrodiesel. Furthermore, results from that study indicated that equations based on second-order polynomial regression analyses were more accurate than semi-logarithmic functions of concentration and v of unblended components.

Subsequently, a second-order polynomial model was applied to data in the present study and results from those regression analyses are summarized in Table 6. As mentioned earlier, data for each set were analyzed based on results for V_{BD} = B0, B4, B8, B12, B16, B20, and B100 blends. These calibrations yielded good results with respect to $R^2 \geq 0.996$ and F ratio ≥ 823; $\sigma_y = 0.61$–2.1 mm^2/s were significantly lower than results from linear regression.

With respect to ULSD, similarities between corresponding A_0, A_1, and A_2 coefficients for SME-1 and SME-2 blends suggested that data sets could be pooled to yield combined expressions for SME/ULSD blends. Data in bold face in Table 6 indicated good results for combined SME blends with respect to $R^2 \geq 0.996$, F ratio $\geq 1{,}456$ and $\sigma_y \leq 2.2$ mm^2/s. In contrast to CP, RI, and SG results, comparing A_0, A_1, and A_2 coefficients for UCOME/ULSD-B blends did not vary greatly with respect to coefficients for SME/ULSD-B blends. Graphical comparison (not shown) indicated some degree of convergence in curves for ULSD-B blends at lower V_{BD}, though the UCOME/ULSD-B curve diverged increasingly as V_{BD} increased from B20 to B100.

Predicting V_{BD} from Property Measurements

Cross-validation graphs for combined SME/ULSD data models developed for CP, RI, SG, and v are shown in Figs. 2, 3, 4, 5. These results clearly indicate that linear models based on SG data provide the strongest correlation between predicted and measured V_{BD}. Regression of results in Fig. 4 yielded (a) slope = 1.003, $R^2 = 0.999$ and $\sigma_y = 1.3$ and (b) slope = 0.987, $R^2 = 0.9992$ and $\sigma_y = 0.88$. Regression of predicted versus measured V_{BD} data for UCOME/ULSD-B blends yielded slope = 1.003, $R^2 = 0.9996$ and $\sigma_y = 0.56$ (graph not shown). Thus, calibration models based on SG data predicted V_{BD} to within 1.3 vol%.

The CP models showed the weakest correlation between predicted and measured V_{BD}. Regression of results in

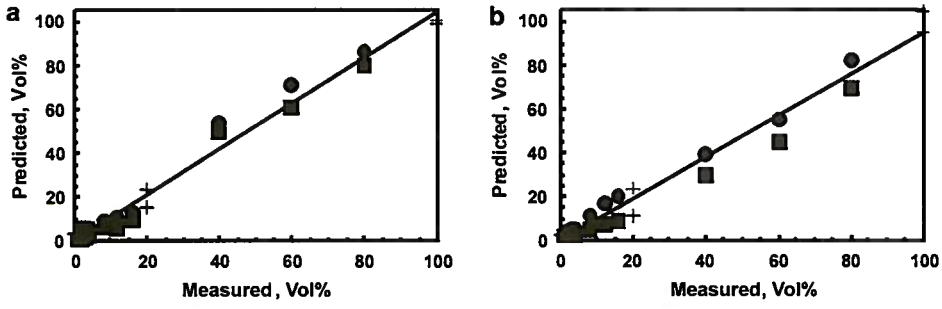

Fig. 2 Cross-validation of linear CP calibration models for **a** Combined SME/ULSD-A blends; and **b** Combined SME/ULSD-B blends. Legend: *plus* = calibration data; *blocked squares* = SME-1 data; *blocked circles* = SME-2 data. See Fig. 1 for abbreviations

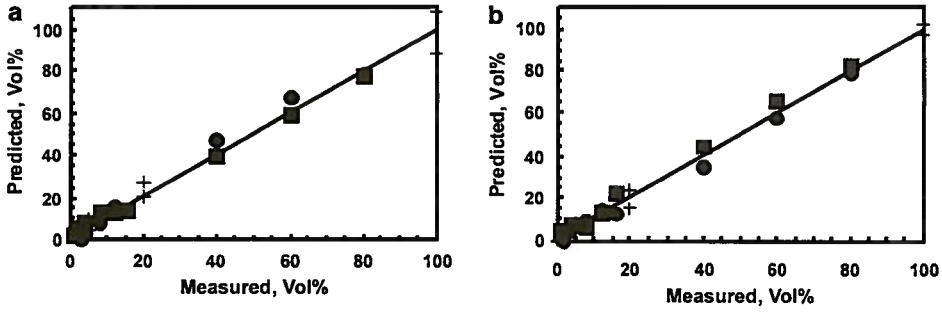

Fig. 3 Cross-validation of linear RI calibration models for **a** Combined SME/ULSD-A blends; and **b** Combined SME/ULSD-B blends. Legend: same as in Fig. 2. See Fig. 1 for abbreviations

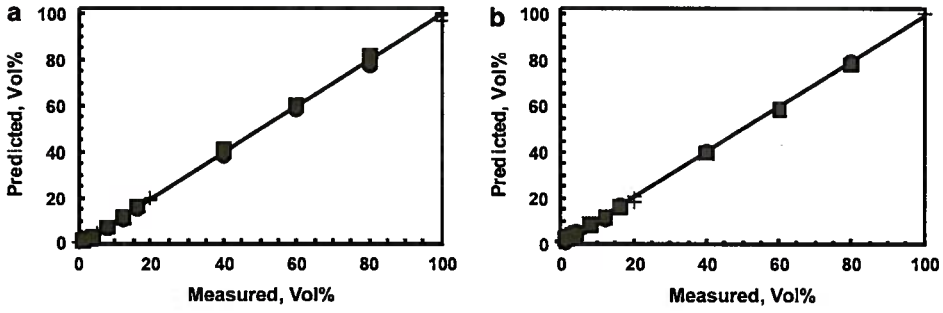

Fig. 4 Cross-validation of linear SG calibration models for **a** Combined SME/ULSD-A blends; and **b** Combined SME/ULSD-B blends. Legend: same as in Fig. 2. See Fig. 1 for abbreviations

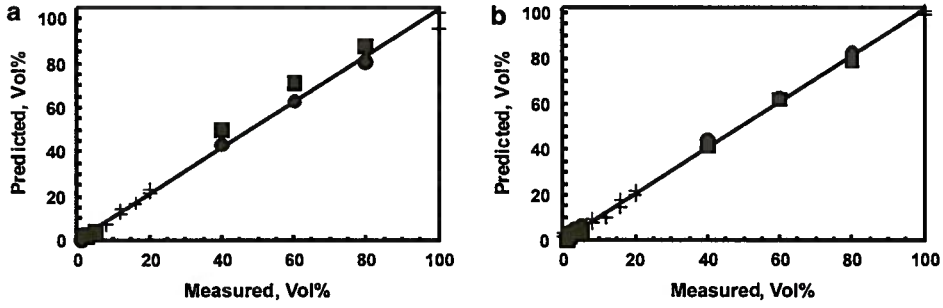

Fig. 5 Cross-validation of second-order polynomial v calibration models for **a** Combined SME/ULSD-A blends; and **b** Combined SME/ULSD-B blends. Legend: same as in Fig. 2. See Fig. 1 for abbreviations

Fig. 2 yielded (a) slope = 1.04, $R^2 = 0.98$ and $\sigma_y = 4.6$ and (b) slope = 0.94, $R^2 = 0.97$ and $\sigma_y = 5.0$. Analysis of UCOME/ULSD-B results yielded slope = 0.98, $R^2 = 0.99$ and $\sigma_y = 3.0$. These data show that although CP has a linear correlation with V_{BD}, it may not predict V_{BD} more accurately than within 5 vol%. Results in Figs. 3 and 5 demonstrated $\sigma_y = 3.0$–4.5 and 1.6–3.2 vol% for predicting V_{BD} from RI and v models.

Correlations were also analyzed for accuracy in predicting V_{BD} of blends defined by two ranges where biodiesel is either an extender (B0, B4, B8, B12, B16, and B20) or an additive (B0, B1, B2, B3, B4, and B5). Accuracy was determined by calculating the root mean square (RMS) deviation in each range by the following equation:

$$\mathrm{RMS} = \sqrt{\frac{1}{n}\sum_{i=1}^{n}\left(V_{BD}^{Calc} - V_{BD}\right)_i^2}$$

where n = number of points and V_{BD}^{Calc} and V_{BD} are predicted and measured values in vol%. Based on SG calibration models, SME/ULSD blends selected in the extender range (B0–B20) yielded RMS = 0.56–1.3 whereas UCOME/ULSD-B blends had RMS = 0.73. Analogous comparison of values from v, RI, and CP models yielded RMS = 0.89–1.9, 0.86–3.9, and 2.5–5.1, respectively. This analysis supports results shown in cross-validation graphs where SG models provided the most accurate prediction of V_{BD} of biodiesel/ULSD blends.

Comparison of predicted and measured V_{BD} values for blends selected in the additive range (B0–B5) yielded RMS = 0.52–0.95 for SG calibration models. Results for v, RI, and CP models yielded RMS = 0.64–3.0, 1.1–3.4, and 1.5–2.8, respectively. Although comparable in magnitude to RMS results for blends selected in the extender range, RMS values for blends in the additive range were more significant (17–113%) relative to the smaller V_{BD} range for comparison. Nevertheless, SG models provided the most accurate prediction of V_{BD} of blends in the additive range.

Finally, models were analyzed for sensitivity to experimental error in measurement of the physical property. This analysis was applied to data for selected blends in extender and additive V_{BD} ranges defined earlier. High and low V_{BD} values were calculated by substituting measured property data into the appropriate model and generating results for each property ± 2(standard deviation); that is, for [property + 2(SD)] and [property − 2(SD)]. For each set of selected biodiesel/ULSD blends, absolute values of the difference between high and low V_{BD} were determined and an average value calculated for that set.

For the extender range, the average difference in calculated V_{BD} were 2.1–8.6, 3.2–26.9, 0.64–2.1, and 0.65–2.9 vol% for CP, RI, SG, and v, respectively. The lowest average differences calculated from SG models were those for SME-1 and SME-2 blends in ULSD-A (0.64 vol%), and from v models was for SME-1/ULSD-B blends (0.65 vol%). In contrast, results from the RI models produced the largest average differences for SME-2/ULSD-A blends (26.9 vol%).

Comparing the average differences for blends selected in the additive range yielded analogous results. Average differences in calculated V_{BD} were 3.3–8.2, 3.2–20.6, 0.64–2.0,

and 0.73–4.6 vol% for CP, RI, SG, and ν. The lowest average differences calculated from SG models were those for SME-1 and SME-2 blends in ULSD-A and from ν models was for SME-1/ULSD-B blends. Results from the RI models produced the largest mean differences for SME-2/ULSD-A blends. Similar to observations made from discussion of RMS data, the magnitude in mean differences for selected blends in the additive range were much higher than those observed for blends in the extender range.

Overall, the present study identifies mathematical models based on linear regression of SG data as the most suitable calibration model for predicting V_{BD} of SME or UCOME blends with ULSD. Secondarily, models based on an empirical second-order polynomial correlation from ν data may be employed to predict V_{BD} of blends, though these calibrations were not as accurate as the SG calibrations. Both SG and ν are cost-effective and can be rapidly measured in the laboratory. These calibrations were more accurate in predicting V_{BD} of blends in the extender range (B0–B20) than the additive range (B0–B5).

In general, calibration models based on physical properties depend significantly on the accuracy of data utilized to generate them. Results in the present study were acquired for blends of well characterized SME, UCOME, and petrodiesel component samples under tightly controlled laboratory conditions. To advance the development of calibration curves based on SG and ν data, future studies will need to be conducted on the properties of blends composed of biodiesel from other producers and feedstocks as well as ULSD from more than two suppliers. In addition, small concentrations of performance-enhancing additives or contaminants such as moisture or free fatty acids may influence SG or ν of biodiesel blends. More studies will be necessary to outline the impact of these materials on the accuracy of predicting V_{BD} of blends from these properties.

Acknowledgments Kim Ascherl, Benetria Banks, Becky Sanders, and Erin Walter prepared and analyzed physical properties of samples in support of the present study.

References

1. Howell S, Jobe J (2010) Biodiesel in the United States. In: Knothe G, Krahl J, Van Gerpen J (eds) The Biodiesel Handbook, 2nd edn. AOCS Press, Urbana, pp 299–314
2. Knothe G, Dunn RO (2005) Biodiesel: an alternative diesel fuel from vegetable oils or animal fats. In: Erhan SZ (ed) Industrial uses of vegetable oils. AOCS Press, Champaign, pp 42–89
3. Knothe G, Dunn RO (2001) Biofuels derived from fats and oils. In: Gunstone FD, Hamilton RJ (eds) Oleochemical manufacture and applications. Sheffield Academic, Sheffield, pp 106–163
4. Van Gerpen JH, Soylu S, Tat ME (1999) Evaluation of the lubricity of soybean oil-based additives in diesel fuels. In: Proceedings of the Annual Meeting of the ASAE. American Society of Agricultural Engineers, St. Joseph (MI), paper no 996314
5. Graboski MS, McCormick RL (1998) Combustion of fat and vegetable oil derived fuels in diesel engines. Prog Energy Combust Sci 24:124–164
6. Schwab AW, Bagby MO, Freedman B (1987) Preparation and properties of diesel fuels from vegetable oils. Fuel 66:1372–1378
7. USEPA (2002) A comprehensive analysis of biodiesel impacts on exhaust emissions. Technical Report No EPA420-P-02-001. US Environmental Protection Agency, Washington (DC)
8. Pradhan A, Shrestha DS, McAloon A, Yee W, Haas M, Duffield JA, Shapouri H (2009) Energy life-cycle assessment of soybean biodiesel. Agricultural economic report no 845. US Department of Agriculture Office of Energy Policy and New Uses, Washington (DC)
9. Huo H, Wang M, Putsche V (2008) Life-cycle assessment of energy and greenhouse gas effects of soybean-derived biodiesel and renewable fuels. Report No ANL/ESD/08–2. Argonne National Laboratory Energy Systems Division, Argonne
10. Elliott DC (2007) Historical developments in hydroprocessing bio-oils. Energy Fuels 21:1792–1815
11. Knothe G, Steidley KR (2005) Lubricity of components of biodiesel and petrodiesel. The origin of biodiesel lubricity. Energy Fuels 19:1192–1200
12. Tang H, Salley SO, Ng KYS (2008) Fuel properties and precipitate formation at low temperature in soy-, cottonseed-, and poultry fat-based biodiesel blends. Fuel 87:3006–3017
13. Tang H, De Guzman RC, Salley SO, Ng KYS (2008) Formation of insolubles in palm oil-, yellow grease-, and soybean oil-based biodiesel blends after cold soaking at 4°C. J Am Oil Chem Soc 85:1173–1182
14. Heck DA, Thaeler J, Howell S, Hayes JA (2009) Quantification of the cold flow properties of biodiesels blended with ULSD. National Biodiesel Board, Jefferson City
15. Knothe G, Steidley KR (2007) Kinematic viscosity of biodiesel components (fatty acid alkyl esters) and related compounds at low temperatures. Fuel 86:2560–2567
16. Tang H, Abunasser N, Wang A, Clark BR, Wadumesthrige K, Zeng S, Kim M, Salley SO, Hirschlieb G, Wilson J, Ng KYS (2008) Quality survey of biodiesel blends sold at retail stations. Fuel 87:2951–2955
17. ASTM (2008) Standard specification for diesel fuel oils. In: Annual Book of ASTM Standards. ASTM International, West Conshohocken (PA), method D 975
18. Heiden RW (1996) Analytical methodologies for the determination of biodiesel ester purity—determination of total methyl esters. Final Report, NBB Contract 520320–1. National Biodiesel Board, Jefferson City
19. Knothe G (2006) Analyzing biodiesel: standards and other methods. J Am Oil Chem Soc 83:823–833
20. Foglia TA, Jones KC, Phillips JG (2005) Determination of biodiesel and triacylglycerols in diesel fuel by LC. Chromatographia 62:115–119
21. Kamifski M, Gilgenast ME, Przyjazny A, Romanik G (2006) Procedure for and results of simultaneous determination of aromatic hydrocarbons and fatty acid methyl esters in diesel fuels by high-performance liquid chromatography. J Chromatogr A 1122:153–160
22. Bírová A, Švijdlenka E, Cvengroš J, Dostálíková V (2002) Determination of the mass fraction of methyl esters in mixed fuels. Eur J Lipid Sci Technol 104:271–277
23. Pimentel MF, Ribeiro GMGS, da Cruz RS, Stragevitch L, Pacheco JGA, Teixeira LSG (2006) Determination of biodiesel content when blended with mineral diesel fuel using infrared spectroscopy and multivariate calibration. Microchem J 82:201–206
24. Knothe G (2001) Determining the blend level of mixtures of biodiesel with conventional diesel fuel by fiber-optic near-

infrared spectroscopy and ^{1}H nuclear magnetic resonance spectroscopy. J Am Oil Chem Soc 78:1025–1028
25. Sanford SD, White JM, Shah PS, Wee C, Valverde MA, Meier GR (2009) Feedstock and biodiesel characteristics report. Renewable Energy Group Inc., Ames
26. ASTM (2008) Standard specification for diesel fuel oil, biodiesel blend (B6–B20). In: Annual Book of ASTM Standards. ASTM International, West Conshohocken (PA), method D 7467
27. Dunn RO (2010) Cold flow properties of biodiesel by automatic and manual analysis methods. J ASTM Int 7(4):1–15 (Paper No JAI102618)
28. ASTM (2009) Standard specification for biodiesel fuel blend stock (B100) for middle distillate fuels. In: Annual book of ASTM standards. ASTM International, West Conshohocken (PA), method D 6751
29. ASTM (2003) Standard test method for cloud point of petroleum products (constant cooling rate method). In: Annual book of ASTM standards. ASTM International, West Conshohocken (PA), method D 5773
30. ASTM (2003) Standard test method for refractive index and refractive dispersion of hydrocarbon liquids. In: Annual book of ASTM standards. ASTM International, West Conshohocken (PA), method D 1218
31. AOCS (1997) Determination of mass per unit volume ("liter weight") in air of oils and fats. In: Firestone D (ed) Official methods and recommended practices of the AOCS, 5th edn. AOCS Press, Champaign method Cc 10c-95
32. ASTM (2003) Standard test method for kinematic viscosity of transparent and opaque liquids (and the calculation of dynamic viscosity). In: Annual book of ASTM standards. ASTM International, West Conshohocken (PA), method D 445
33. Knothe G, Dunn RO (2009) A comprehensive evaluation of the melting points of fatty acids and esters determined by differential scanning calorimetry. J Am Oil Chem Soc 86:843–856
34. Dunn RO, Bagby MO (1995) Low-temperature properties of triglyceride-based diesel fuels: transesterified methyl esters and petroleum middle distillate/ester blends. J Am Oil Chem Soc 72:895–904
35. Schumacher L, Chellappa A, Wetherell W, Russell MD (1995) The physical & chemical characterization of biodiesel low sulfur diesel fuel blends (final report). National Biodiesel Board, Jefferson City
36. Joshi RM, Pegg MJ (2007) Flow properties of biodiesel fuel blends at low temperatures. Fuel 86:143–151
37. Benjumea P, Agudelo J, Agudelo A (2008) Basic properties of palm oil biodiesel-diesel blends. Fuel 87:2069–2075
38. Waynick JA (2005) Characterization of biodiesel oxidation and oxidation products. Report for CRC Project No AVFL-2b. The Coordinating Research Council, Apharetta (GA)
39. Alptekin E, Canakci M (2008) Determination of the density and the viscosities of biodiesel-diesel fuel blends. Renewable Energy 33:2623–2630
40. Yuan W, Hansen AC, Zhang Q, Tan Z (2005) Temperature-dependent kinematic viscosity of selected biodiesel fuels and blends with diesel fuel. J Am Oil Chem Soc 82:195–199